

Pressure effect on the energy structure and superexchange interaction of the undoped orthorhombic La_2CuO_4 : beyond the low-energy approximation

Vladimir A. Gavrichkov,^{1,2} Zlata V. Pchelkina,^{3,4} Igor A. Nekrasov,⁵ and Sergey G. Ovchinnikov^{1,2}

¹*L. V. Kirensky Institute of Physics, Siberian Branch of Russian Academy of Sciences, 660036, Krasnoyarsk, Russia*

²*Siberian Federal University, 660041, Krasnoyarsk, Russia*

³*Institute of Metal Physics, Ural Branch of the Russian Academy of Sciences, 620219, Ekaterinburg, Russia*

⁴*Theoretical Physics and Applied Mathematics Department,
Ural Federal University, 620002 Ekaterinburg, Russia*

⁵*Institute of Electrophysics, Ural Branch, Russian Academy of Sciences, 620016, Ekaterinburg, Russia*

(Dated: February 10, 2018)

Using LDA+GTB multi-band approach, we studied the compression dependence of the electronic structure and in-plane superexchange interaction $J(P)$ in the antiferromagnetic La214 at the 0% and 3% - hydrostatic and uniaxial (along c axial) compression. We obtained the superexchange interaction $J(P=0) \approx 0.15\text{eV}$ is enhanced by $\sim 20\%$ under the 3% - hydrostatic compression and vice versa the $J(P)$ is decreased slightly by $\sim 5,7\%$ under the 3% - uniaxial compression. In both cases the $J(P)$ correlates with the in-plane hopping parameters and dd -excitation energy $\delta_s = \varepsilon(^3B_1) - \varepsilon(A_1)$ involving the two-hole states: Zhang-Rice singlet and 3B_1 triplet states. The spectral density of the first removal states is a combined singlet-triplet character and a sign of changes in the one with the pressure clearly reproduces the \vec{k} -distribution of quasiparticle states with a different a_1 - and b_1 -symmetry over the Brillouin zone as a whole.

PACS numbers: 75.30.Et 74.62.Fj 74.72.Cj

I. INTRODUCTION

A superexchange study in the high T_c cuprates is an important part in the bosonic battle: ¹⁻⁸ magnetic or lattice - what are relevant to pairing? The studies of the different pressure dependences of critical temperature $T_C(P)$ observed universal trend: $\partial T_C/P_c < 0$ and $\partial T_C/P > 0$ ⁹ for an anisotropic and isotropic pressures respectively. A correlation between the Cu- O_{ap} apical bond distance and T_c in the cuprates has been found by Jorgensen and co-workers. ¹⁰ The Cu- O_{ap} apical bond distance increases with the c -axis length. The role of the apical oxygen on the electronic properties has also been addressed in several theoretical works ¹¹⁻¹⁴ which all find that T_c is highest for materials in which the apical bond distance is large. The Y-123, where contrary to the general trend for cuprates, T_c increased against the contraction along all the crystal axes, is the exception. Due to a presence of CuO chains its behavior is unusual, and not representative of the cuprates as a whole. ⁹

Recently, the time-frequency resolved spectroscopy ¹⁵ has shown the dominant role of the non-redarding electronic mechanism of pairing in optimally doped Bi-cuprate. The exchange magnetic interaction is one of the candidates for electronic pairing. At the same time the experimental studies ¹⁶⁻¹⁸ show increasing superexchange $\partial J/\partial P > 0$ under hydrostatic pressure P . However, we didn't find any publication on the J dependence on uniaxial pressure.

Our theoretical work will be devoted the issue that could not be solved at low-energy limit: the superexchange interaction and as an example its different pressure dependences $J(P)$ in the undoped La214. This phenomena cannot be understood relying only on the low-

energy approximation (in the framework of the three-orbital pd -model). ^{19,20} The value of superexchange interaction J in the La214 is controlled by a large number of excited two hole states: N_T triplets and N_S singlets including the Zhang-Rice state A_1 .

Essentially, there are two acceptable approaches to the study of superexchange interaction. The first is the calculation with the intermediate two-hole states which arise through hopping from oxygen to oxygen in the perturbation theory of a higher order than a fourth. ²¹ Another approach is a cell perturbation theory taking into account all of the excited states. The latter seems more appropriate, ²¹⁻²³ where, however, it is necessary to work with a large number of excited states. ²⁴ Especially, if we keep in mind that the energy gap in the La214 between the A_1 singlet and 3B_1 triplet two-hole cell states involving Cu- d_{z^2} and O_{ap} - p_z apical oxygen states can be quite small. ²⁵⁻²⁹

Using the LDA+GTB approach ³⁰ which extends the cell perturbation theory ^{22,23} to an arbitrary number of the excited cell states, we calculate the compression dependence of superexchange constant $J(P)$ in the orthorhombic La214, where unlike the pressure dependencies of superexchange interaction in many other conventional transition-metal oxide, ³¹⁻³⁴ the two-magnon Raman scattering experiments show that $J(P)$ has a substantially weaker pressure dependence. ¹⁶⁻¹⁸ Within the perturbation theory using the atomic orbitals representation, ^{21,35,36} a superexchange interaction is obtained at the fourth-order of a perturbation theory and the weak-pressure dependence of $J(P)$ is clearly not consistent with the pressure dependencies of the main parameters of the pd -model: $t_{pd} \sim a^{-\alpha}$ ($2.5 \lesssim \alpha \lesssim 3.0$), ³⁷⁻⁴⁰ $\Delta \sim a^{-\beta}$ ($\beta \approx 0.4 \pm 0.4$). ⁴¹ Comparison of

the results at the the fourth-order with the calculations in higher orders of perturbation theory²¹ and the exact diagonalization of finite clusters^{12,21,42-44} shows that the in-plane superexchange J depends on the t_{pd} significantly weaker and, because of the too large value of t_{pd}/Δ in the CuO_2 layer, the fourth order may be insufficient.

We discuss the exchange constant J , and compare our results with the conclusion from the neutron experiments in undeformed La214,⁴⁵ the experiments related to the two-magnon Raman scattering in deformed materials¹⁶ at the 0%, 3% hydrostatic and uniaxial (along c axis) compressions.

One of the features of the study is that the exchange interaction is derived from the original electronic structure of material, and we can compare a compression effect on the superexchange interaction with a same effect on the electronic structure. All related changes in the electronic structure of a material under pressure is also available to study.

At a fixed energy of the incident photons a photocurrent I in the unpolarized ARPES experiments is proportional to the partial contribution of the spectral density from electron orbital λ :

$$I(\vec{k}, E, P) \sim I_0(\vec{k}, P) f_F(E) \sum_{\lambda} A_{\lambda}(\vec{k}, E, P), \quad (1)$$

where $A_{\lambda}(\vec{k}, E, P)$, $f_F(E)$, $I_0(\vec{k}, P)$ are the partial spectral density from the λ -orbital, the Fermi function and the matrix element of the interaction of electron with the incident photons respectively. Over a pressure range where a crystal symmetry is unchanged, the matrix element $I_0(\vec{k}, P) \approx I_0(\vec{k})$, i.e. the relative changes of the photocurrent $\delta I(\vec{k}, E, P)$ with a pressure are caused by the changes in the spectral intensity $\delta A_{tot}(\vec{k}, E, P) = A_{tot}(\vec{k}, E, P) - A_{tot}(\vec{k}, E)$, where $A_{tot}(\vec{k}, E, P) = \sum_{\lambda} A_{\lambda}(\vec{k}, E, P)$.

In this work, we study the compressure effects on the $A_{tot}(\vec{k}, E, P)$ along with changes in the superexchange interaction $J(P)$ in a framework of the five orbital model where the orbital index λ corresponds either to the $\text{Cu}3d$ orbitals $d_{x^2-y^2}$ and $d_{3z^2-r^2}$ or to symmetrized combinations of the $\text{O-}2p^{\sigma}$ atomic orbitals centered at the copper site \vec{R}_f : b, a orbitals (transforming like b_1 and a_1),²³ $\text{O}_{ap-}2p_z$. To specify partial contribution $A_{b_1} = \sum_{\lambda} A_{\lambda}(P)$ and $A_{a_1} = \sum_{\lambda'} A_{\lambda'}(P)$ to the $A_{tot}(\vec{k}, E, P)$ -total spectral density of the first removal electron state (frs) in the undoped antiferromagnetic La214, we also studied compression dependence of the partial contributions. In line with our results the spectral density from b_1 - and a_1 -symmetry quasiparticle (qp -) states extends along the edges of the AFM Brillouin zone and the near the \vec{k} -points: $(0, 0)$, (π, π) respectively. The sign of the pressure effects on the total spectral density $\delta A_{tot}(\vec{k}, E, P)$

provides a clear imprints of the b_1 - and a_1 - contributions to the frs -state over the Brillouin zone as a whole.

We obtained that the superexchange constant in the undeformed La214 is close to the experimental value 0.146 eV ⁴⁵ and increases by $\sim 20\%$ under 3%-hydrostatic compression. At the same time, the superexchange interaction is only slightly reduced by $\sim -5.7\%$ under the uniaxial compression. According to the available experimental results,¹⁶ the superexchange interaction is increased by $\sim 18\%$ at 3%-hydrostatic compression ($P \sim 205\text{Kbar}$). In both cases, the hydrostatic and anisotropic compression the $J(P)$ correlates with the energy $\delta_s = \varepsilon(^3B_1) - \varepsilon(A_1)$ of dd -excitation involving the the two-hole states: Zhang-Rice state A_1 and triplet state 3B_1 . Showing with the $T_c(P)$ the similar trend: $\partial J/\partial P > 0$ and $\partial J/\partial P_c < 0$ the $J(P)$ dependence support the magnetic view of a discussion on pairing mechanism at least in the single layer cuprates.

We also carried out the GTB calculation of a hypothetical case of the $A_1 \leftrightarrow ^3B_1$ two-hole state crossover. Due to the orbital features of Zhang-Rice state the superexchange keeps the antiferromagnetic character even at such a hypothetical set of the parameters of Hamiltonian.

II. ALL VALENCE STATES IN MULTIBAND pd -MODEL

In the multiband pd -model,⁴⁶ a Hamiltonian includes the local energies of holes for the oxygen and copper at the different orbital states, the intraatomic Coulomb and exchange interactions for copper and oxygen, hoppings, and the copper-oxygen Coulomb interaction. The important difference with the low energy three orbital pd -model^{19,20} is related to an addition of the z -oriented d_{z^2} orbital of copper and p_z orbital of the apical oxygen ions. In the framework of the local density approximation in combination with the generalized tight-binding method (LDA+GTB), the Hamiltonian parameters are calculated from first principles.⁴⁷ Then, the cell approach of the generalized tight-binding method^{30,48} is used to take into account strong electron correlations explicitly. A crystal lattice is divided into unit cells, so that the Hamiltonian is represented by $H_0 + H_1$, where the component H_0 is the sum of intracell terms and the component H_1 takes into account the intercell hoppings and interactions. The component H_0 is exactly diagonalized. The exact multielectron cell states $|n, \nu\rangle$ and energies $\xi_{n\theta}$ are determined. Then these states are used to construct the Hubbard operators of the unit cell \vec{R}_f : $X_f^{n\theta, n'\theta'} = |n\theta\rangle\langle n'\theta'|$, where $\theta = S(0), M(-1, 0, +1)$ for the singlet and triplet states respectively, the index n is the sequence number of doublet state in the one-hole sector $n_h = 1$ and also singlet, triplet states in the two-hole sector $n_h = 2$ (Fig.1). Thereafter, the component H_1 is exactly written in the X -operator representation and the intercell interactions are included in terms of the perturbation theory. The

procedure and results of calculations for the undeformed CuO₂ layer are described in our previous review paper.³⁰

$$H_0 = \sum_f \left\{ \varepsilon_0 X_f^{00} + \sum_{l\sigma} (\varepsilon_l - \mu) X_f^{l\sigma, l\sigma} + \left[\sum_{n=1}^{N_S} (E_{nS} - 2\mu) X_f^{nS, nS} + \sum_{m=1}^{N_T} \sum_M (E_{mM} - 2\mu) X_f^{mM, mM} \right] \right\}, \quad (2)$$

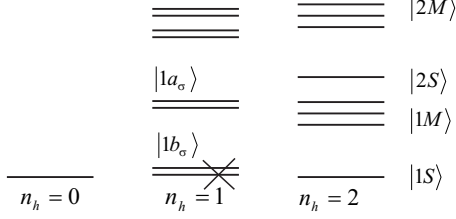


FIG. 1. Energy-level scheme of the Hilbert space of the CuO₆ unit cell with the numbers of holes $n_h = 0, 1,$ and 2 . The cross indicates the occupied ground state $|1b_\sigma\rangle$ of the configuration $d^9 p^6 + d^{10} p^5$ in the undoped case.

where ε_0 is the energy of the "vacuum" term $d^{10} p^6$ in the hole representation, ε_l is the energy of one-hole molecular orbitals with the spin projections $\sigma = \pm 1/2$, and the index l runs over all one-particle states of the CuO₆ cluster. The term in square brackets in (2) describes the contributions from two-hole singlet states $|n, S\rangle$ and the triplet states $|m, M\rangle$. The indices $n(1 \leq n \leq N_S)$ and $m(1 \leq m \leq N_T)$ numerate all two-hole spin singlets and triplets respectively. A completeness of the set of local Hubbard operators is represented by the sum:

$$X_f^{00} + \sum_{l\sigma} X_f^{l\sigma, l\sigma} + \sum_n X_f^{nS, nS} + \sum_m \sum_M X_f^{mM, mM} = 1. \quad (3)$$

The energy-level scheme of the many-electron terms of the H_0 for the La214 compound is depicted in Fig.1. A creation of an electron at the bottom of the conduction band is determined by the matrix element $\gamma_{\lambda\sigma}(0) = \langle 0 | a_{f\lambda\sigma} | b_\sigma \rangle$. A creation of the hole upon p -type doping is determined by the matrix elements with the participation of all two-hole terms:

$$\gamma_{\lambda\sigma}(n) = \langle b_\sigma | a_{f\lambda\sigma} | ns \rangle,$$

$$\gamma_{\lambda\sigma}(m) = \langle b_\sigma | a_{f\lambda\sigma} | m, +2\sigma \rangle. \quad (4)$$

In the X-operator representation the component H_0 is determined by the sum over the unit cells, that is

In the X-operator representation, the hole annihilation operator has the form

$$a_{f\lambda\sigma} = \gamma_{\lambda\sigma}(0) X_f^{0, \sigma} + \sum_n \gamma_{\lambda\sigma}(n) X_f^{\bar{\sigma}, ns} + \sum_m \gamma_{\lambda\sigma}(m) \left(X_f^{\sigma, m2\sigma} + \frac{1}{\sqrt{2}} X_f^{\bar{\sigma}, m0} \right). \quad (5)$$

Forming the singlet and triplet Hubbard subbands with a hybridization between them the two-hole states with nonzero matrix elements (4) are involved to a formation of the valence band energy structure. It should be noted that the singlet (triplet) band is a conventional name for designation of the electronic band with the spin $\sigma = 1/2$ but with a participation of final singlet (triplet) terms. A representation of the off-diagonal operators X can be simplified by introducing the root vectors $\vec{\alpha}_r(n\theta, n'\theta')$ corresponding to a pair of the initial and final states. In this notation, the last relationship takes the form $a_{f\lambda\sigma} = \sum_r \gamma_{\lambda\sigma}(r) X_f^r$ where the integer index r numbers all one-particle excitations:

$$\{\vec{\alpha}_r\} = \{(0, l\sigma); (l\sigma, ns); (l\sigma, m2\sigma'); (l\sigma, m0)\}. \quad (6)$$

Moreover, in the same notation, the Hamiltonian of the intercluster hopping has the simple form

$$H_1 = \sum_{fg} \sum_{\lambda\lambda'\sigma} t_{fg}^{\lambda\lambda'} a_{g\lambda\sigma}^+ a_{f\lambda'\sigma} + h.c. = \sum_{fg} \sum_{rr'} t_{fg}^{rr'} X_f^r X_g^{r'}, \quad (7)$$

where $t_{fg}^{\lambda\lambda'}$ is the matrix of hopping integrals of a hole from the g -th cell (in the orbital state λ') to the f -th cell (in the orbital state λ) and

$$t_{fg}^{rr'} = \sum_{\lambda\lambda'} \sum_{\sigma} t_{fg}^{\lambda\lambda'} \times [\gamma_{\lambda\sigma}^*(r) \gamma_{\lambda'\sigma}(r') + \gamma_{\lambda'\sigma}^*(r) \gamma_{\lambda\sigma}(r')]. \quad (8)$$

Since each index r characterizes the band of quasiparticles in a strongly correlated system (the Hubbard band index), the diagonal terms t^{rr} in the last expression describe the dispersion of the r -th band and the off-diagonal terms $t^{rr'}$ describe the hybridization of the r -th and r' -th bands. The equations of motion for the Green's function can be solved within the different approximations. In the diagram technique for X -operators⁴⁹ with the intercell hopping H_1 as a perturbation the Hartree-Fock approximation results in the Hubbard-I type solution

$$D_{\vec{k}}^{rr'} = \delta_{rr'} \delta_{fg} D_r^{(0)} + D_r^{(0)} \sum_{\lambda\lambda'} \sum_{r''} t_{\lambda\lambda'}(\vec{k}) \{ \gamma_{\lambda\sigma}^*(r) \gamma_{\lambda'\sigma}(r'') + \gamma_{\lambda'\sigma}^*(r) \gamma_{\lambda\sigma}(r'') \} D_{\vec{k}}^{r''r'}, \quad (9)$$

where $t_{\lambda\lambda'}(\vec{k}) = \sum_{\vec{h}} t_{\lambda\lambda'}(\vec{h}) e^{i\vec{k}\vec{h}}$. We can use the matrix notation

$$\hat{D}_{\vec{k}} = \hat{\Pi}^{-1}(\vec{k}) \hat{D}^{(0)}, \quad (10)$$

where $\hat{\Pi}(\vec{k}) = 1 - \hat{D}^{(0)} \hat{t}(\vec{k})$ and

$$D_{0fg}^{rr'} = \delta_{fg} \delta_{rr'} \frac{F(r)}{E - \Omega_r}, \quad (11)$$

$F(r) = \langle X_f^{n\theta, n\theta} + X_f^{n'\theta', n'\theta'} \rangle$ and $\Omega_r = \Omega(\vec{\alpha}_r) = \xi_{n\theta} - \xi_{n'\theta'}$. Thus the dispersion relations of the quasiparticles are determined by an equation on the poles of matrix Green function $\hat{D}_{\vec{k}}$:

$$\left\| (E - \Omega_r) \delta_{rr'} - F(r) t^{rr'}(\vec{k}) \right\| = 0. \quad (12)$$

Each r -th root vector defines the Fermi excitation in multielectron system of the CuO₂ layer - quasiparticle with charge e , spin 1/2, and local energy Ω_r . Table I shows the values of hopping parameters and single electron energies for orthorhombic La214 obtained in the frameworks of Wannier function projection procedure for different sets of trial orbitals⁴⁷ at zero, 3% - hydrostatic and uniaxial compressions. Despite the fact that the table shows the same vector, a system of the connecting vectors varies slightly with increasing compression, and a volume of the unit cell under uniaxial compressure was assumed a constant.

In the Russell-Saunders scheme all the possible solutions $E_{rk\sigma}$ are classified according to spin σ of the quasiparticle and the number of solutions is equal to twice the number of root vectors r : $2N$, where $N = N_S + 3N_T$. Because of a spin degeneracy of the ground state of the AFM in the single-hole sector, there is a symmetry in the $E_{rk\sigma}$ with respect to the replacement $\sigma \leftrightarrow \bar{\sigma}$. The $E_{r=0k\sigma}$ -energy position of the qp -peak of the frs -state corresponds to the solution with the lowest energy in a hole representation. A spectral density of the qp -states (amplitude of the qp -peak) in turn is determined by the single-particle Green's function

$$A_{tot}(\vec{k}, E, P) = \left(-\frac{1}{\pi} \right) \sum_{\lambda, \sigma} \gamma_{\lambda\sigma}(r) \gamma_{\lambda\sigma}^*(r') \text{Im} D_{\vec{k}}^{rr'}. \quad (13)$$

According to the equations (12) and (13) the $A_{tot}(\vec{k}, E = E_{0\vec{k}\sigma})$ - amplitude and $E_{0k\sigma}$ - energy position of a qp -peak for the frs -state in the undeformed AFM La214 behaves as follows (Fig.2). The frs -state has a mixed singlet-triplet character with the \vec{k} -depending amplitude of a qp -peak. The latter has a maximum value along

the antiferromagnetic Brillouin zone edges, because the number of qp -states in the initial singlet and triplet bands differs significantly. Under hydrostatic compressure the frs -band width increases and amplitude of a qp -peak near the \vec{k} -points $(0,0)$ and (π, π) significantly attenuated (see $\delta A_{tot}(P)$ and $\delta E_{0\vec{k}\sigma}(P) = E_{0\vec{k}\sigma}(P) - E_{0\vec{k}\sigma}(0)$ on Fig. 3,(a) and (b)). Under uniaxial compressure the frs -band width decreases and amplitude of a qp -peak near the \vec{k} -points $(0,0)$ and (π, π) is increased. As consequence, the total spectral density over the Brillouin zone is leveled (Fig. 3, (c) and (d)). A significant contribution of the a_1 -orbital group at the $(0,0)$ and (π, π) \vec{k} -points of Brillouin zone is a reason of this spectral intensity behavior.

III. EFFECTIVE SUPEREXCHANGE HAMILTONIAN

The superexchange interaction appears at the second order of the cell perturbation theory with respect to hoppings.²² That corresponds to virtual excitations from the occupied singlet and triplet bands through the insulating gap to the conduction band at the root vector $r = 0$, $\alpha_0 = (0, \sigma)$ and back (Fig.4). These perturbations are described by the off-diagonal elements t_{fg}^{0r} with $r \geq 1$ in expression (8). In the Hubbard model, there is only one such element t^{01} , which describes the hoppings between the lower and upper Hubbard bands. In our case, the set of nonzero matrix elements $\gamma_{\lambda\sigma}(r)$ with $r \geq 1$ determines the interband hoppings. In order to eliminate them, we generalize the projection operator method proposed by Chao et al⁵⁰ to the Hubbard model. Since the diagonal Hubbard operators are projection operators, the X -operator representation allows us to construct this generalization. In our case the total number of diagonal two-hole operators $X_f^{\mu\mu}$ is equal to N and the sequence index μ ($1 \leq \mu \leq N$) runs over all the two-hole states.

By disregarding the exponentially low temperature occupation of excited one-hole terms in the absence of doping when none of the two-hole state is occupied, we can retain only one lower one-hole state $|1b_\sigma\rangle$ marked by the cross in Fig.1. Further we will omit the index $1b$ in the set of root vectors (6).

We choose a pair of neighboring cells (i, j) and construct the set of projection operators p_μ :

$$p_0 = \left(X_i^{00} + \sum_{\sigma} X_i^{\sigma\sigma} \right) \left(X_j^{00} + \sum_{\sigma} X_j^{\sigma\sigma} \right), \quad (14)$$

$$p_\mu = X_i^{\mu\mu} + X_j^{\mu\mu} - X_i^{\mu\mu} \sum_{\nu} X_j^{\nu\nu}. \quad (15)$$

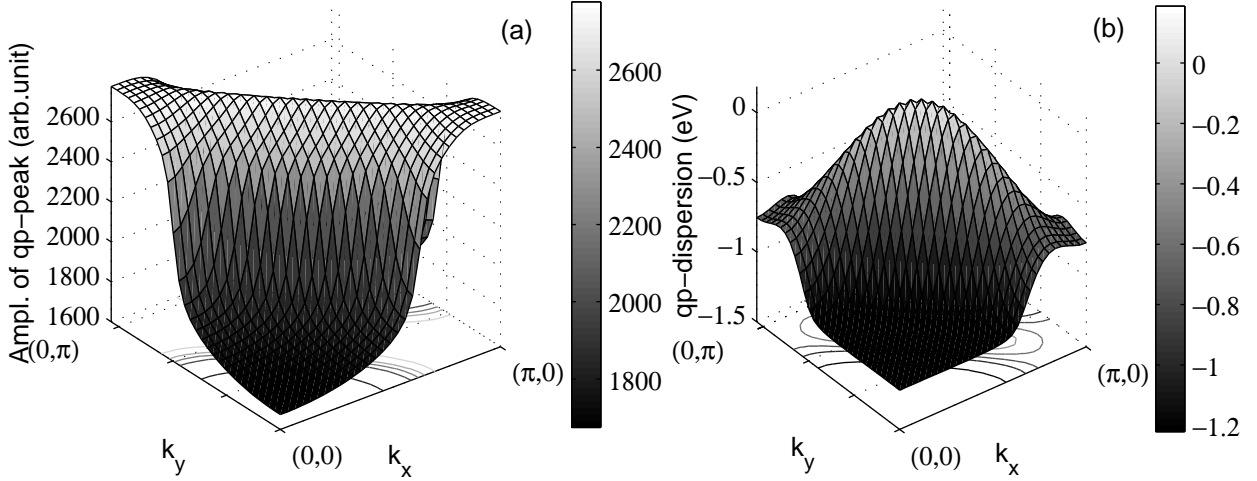


FIG. 2. (a): \vec{k} - dependencies of the qp -peak amplitude $A_{tot}(\vec{k}, E_{0\vec{k}\sigma})$ and (b): qp -peak position $E_{0\vec{k}\sigma}$ of the first removal electron states in the undeformed La214

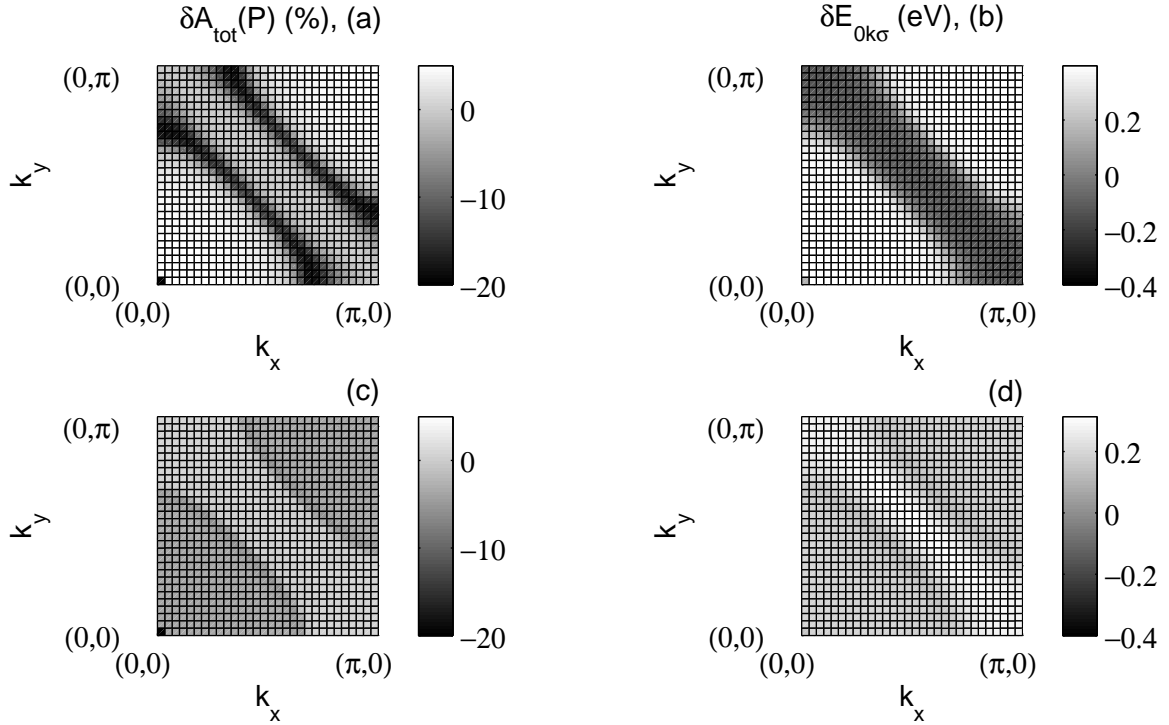


FIG. 3. (a) and (c): \vec{k} - dependence of the $\delta A_{tot}(P)$ -relative changes in a spectral intensity at the 3% - hydrostatic and uniaxial compressions respectively, (b) and (d): \vec{k} - dependence of the $\delta E_{0\vec{k}\sigma}$ -changes in the qp -peak position at the 3% - hydrostatic and uniaxial compressions respectively.

It is easy to check that each operator p_μ is a projection operator $p_\mu^2 = p_\mu$, and these operators form a complete system and are orthogonal, $p_\mu p_\nu = \delta_{\mu\nu} p_\mu$, $\sum_{\mu=0}^N p_\mu = 1$.

By using the identity

$$H = \sum_{\mu\nu} p_\mu H p_\nu, \quad (16)$$

we calculate the diagonal and off-diagonal matrix elements (16). The term $p_0 H p_0$ corresponds to the Hamiltonian component acting in the Hubbard band at the

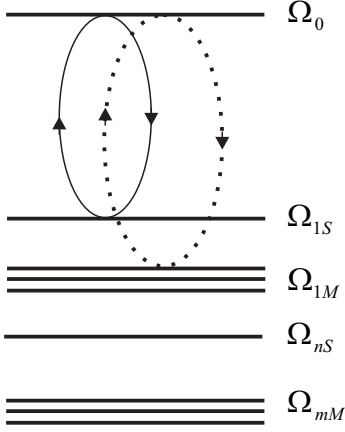


FIG. 4. The virtual excitations from the occupied valence band states into the empty conductivity band and back that results in the superexchange interaction in La214. Solid line corresponds to the antiferromagnetic contribution forming by the singlet bands, and dotted line denotes the ferromagnetic contribution of triplet bands

root vector $\alpha_0 = (0, \sigma)$, etc. It is easy to show that the equality

$$\sum_{\mu} p_{\mu} H_0 p_{\mu} = H_0 \quad (17)$$

is satisfied and that the diagonal elements $p_{\mu} H_1 p_{\mu}$ describe the hoppings in the band μ and the off-diagonal elements $p_{\mu} H_1 p_{\nu}$ correspond to the hybridization of the bands μ and ν . We introduce the small parameter $\varepsilon \ll 1$ and Hamiltonian $\tilde{H}(\varepsilon)$ as

$$\begin{aligned} \tilde{H}(\varepsilon) &= \tilde{H}_0 + \varepsilon \tilde{H}_1, \\ \tilde{H}_0 &= \sum_{\mu} p_{\mu} H p_{\mu}, \quad \tilde{H}_1 = \sum_{\mu\nu} p_{\mu} H p_{\nu} \end{aligned} \quad (18)$$

$$\begin{aligned} H'(\varepsilon = 1) &= \sum_{\mu} p_{\mu} H p_{\mu} + \frac{1}{2} \sum_{\nu \neq \mu} (p_{\mu} H p_{\nu} S - S p_{\mu} H p_{\nu}) \\ &= \sum_{\mu} p_{\mu} H p_{\mu} - \frac{1}{2} \sum_{\mu \neq \nu} \left\{ \frac{[p_{\mu} H p_{\nu}, p_{\nu} H p_{\mu}]_{-}}{\Delta_{\mu\nu}} + \sum_{\substack{\alpha \neq \mu \\ \alpha \neq \nu}} \left[\frac{(p_{\mu} H p_{\nu})(p_{\nu} H p_{\alpha})}{\Delta_{\nu\alpha}} - \frac{(p_{\alpha} H p_{\mu})(p_{\mu} H p_{\nu})}{\Delta_{\alpha\mu}} \right] \right\}. \end{aligned} \quad (24)$$

The calculation of the terms in Hamiltonian (24) for the singlet and triplet bands leads to different results. The interband transitions through the gap are described by the commutator

$$[p_0 H p_{\nu}, p_{\nu} H p_0]_{-}. \quad (25)$$

For the n -th singlet band at the root vector $\vec{\alpha}_{\nu} = (\bar{\sigma}, nS)$,

with the perturbation - interband part \tilde{H}_1 . We also perform the standard unitary transformation

$$H'(\varepsilon) = e^{-i\varepsilon S} \tilde{H}(\varepsilon) e^{i\varepsilon S} \quad (19)$$

to eliminate the linear (over ε) contributions to \tilde{H}_1 . If the matrix \hat{S} satisfies the equation

$$\tilde{H}_1 + i[\tilde{H}_0, S]_{-} = 0. \quad (20)$$

The transformed Hamiltonian are given by

$$H'(\varepsilon) = \tilde{H}_0 + i\varepsilon^2 [\tilde{H}_1, S]_{-} / 2. \quad (21)$$

In order to solve (20), we multiply each term by p_{μ} from the left and by p_{ν} from the right. As a result, we obtain

$$\begin{aligned} p_{\mu} H p_{\nu} (1 - \delta_{\mu\nu}) + i(p_{\mu} H p_{\mu})(p_{\mu} S p_{\nu}) \\ - i(p_{\mu} S p_{\nu})(p_{\nu} H p_{\nu}) = 0. \end{aligned} \quad (22)$$

This equation coincides in form with the corresponding equation in the work ⁵⁰ and differs from it only in the dimension of matrices. Therefore, our derivation of the system of operators p_{μ} in the multiband case is actually a generalization of the method proposed in the work. ⁵⁰ It follows from (22) that the diagonal matrix elements have the form $p_{\mu} S p_{\mu} = \eta p_{\mu}$, where η is a constant. In order to solve the equation with respect to the off-diagonal elements $p_{\mu} S p_{\nu}$, according to ⁵⁰, we make the approximation $p_{\mu} H p_{\mu} \rightarrow \varepsilon_{\mu}$. As a result, the solution has the form

$$p_{\mu} S p_{\nu} = i p_{\mu} H p_{\nu} / \Delta_{\mu\nu}, \quad \Delta_{\mu\nu} = \xi_{\mu} - \xi_{\nu}, \quad (23)$$

where the ξ_{μ} is an energy of μ -th eigen state of the H_0 (2). The effective Hamiltonian is represented as

commutator (25) is determined by the operators

$$\sum_{fgij} \sum_{\sigma\sigma'} [X_f^{\sigma 0} X_g^{-\sigma, ns}, X_i^{ns, -\sigma'} X_j^{0\sigma'}]_{-}. \quad (26)$$

The exchange contribution to the Heisenberg Hamiltonian has the form

$$H_A = \sum_{ij} J_A (\vec{R}_{ij}) (\vec{s}_i \vec{s}_j - \frac{1}{4} n_i n_j), \quad (27)$$

where \vec{s} and n_i are the spin operators for $s = 1/2$ and

the number of particles at the i -th site, respectively, and

$$J_A(\vec{R}_{ij}) = \sum_n J_A^{(n)}(\vec{R}_{ij}) = \sum_{n=1}^{N_s} |t_{ij}^{0,ns}|^2 / \Delta_{ns},$$

$$\Delta_{ns} = E_{ns} - 2\epsilon_1. \quad (28)$$

For the m -th triplet band, commutator (25) is determined by the terms

$$\left[X_f^{\sigma;0} \left(X_g^{\sigma;-m,2\sigma} + \frac{1}{\sqrt{2}} X_g^{-\sigma;m,0} \right) \left(X_i^{m,2\sigma';\sigma'} + \frac{1}{\sqrt{2}} X_i^{m,0;-\sigma'} \right) X_j^{0;\sigma'} \right]. \quad (29)$$

The ferromagnetic exchange contribution to the Heisenberg Hamiltonian takes the form

$$H_F = \sum_{ij} J_B(\vec{R}_{ij}) (\vec{s}_i \vec{s}_j + \frac{3}{4} n_i n_j), \quad (30)$$

where $J_B(\vec{R}_{ij}) = \sum_m J_B^{(m)}(\vec{R}_{ij}) = - \sum_{m=1}^{N_T} |t_{ij}^{0,m}|^2 / 2\Delta_m$ and $\Delta_m = E_m - 2\epsilon_1$. By summing up over all singlet and triplet bands, we find the following expression for the effective exchange interaction parameter:

$$J_{ij} = \sum_{n=1}^{N_s} |t_{ij}^{0,ns}|^2 / \Delta_{ns} - \sum_{m=1}^{N_T} |t_{ij}^{0,m}|^2 / 2\Delta_m. \quad (31)$$

The origin of the antiferromagnetic contribution resulting from the lowest Zhang-Rice and all excited singlet states is the same as in Hubbard model, it is the superexchange. High energy excited states gives less contribution to the total exchange parameter due to the energy denominator. Nevertheless the number of excited singlets in our five orbital approach $N_S = 15$ and triplet $N_T = 10$.

IV. COMPRESSION DEPENDENCE OF THE SUPEREXCHANGE INTERACTION

A penultimate line in Tab.I shows the superexchange constant $J(P)$ calculated by the formula (31) at the five orbital approach. The calculations show that the $J(P)$ increases by $\sim 20\%$ under hydrostatic 3%-compression. This result can be compared with experimental results¹⁶ obtained for the La214. Under the hydrostatic 100Kbar pressure the r_{Cu-O} reduces by $\sim -2\%$, while the J increases by $\sim 10\%$. There are also studies where the linear dependence of the superexchange on the pressure was observed up to a $P = 410$ Kbar.¹⁷ According to the dependence of the La214 crystal structure on the pressure we can find the pressure $P \sim 205$ Kbar corresponds to the 3%-deformed material.⁵¹ The $J(P)$ at this pressure increases by $\sim 18\%$.¹⁷ The calculated value $J \approx 0.15$ eV in the undeformed La214 exceeds the $0.1eV \div 0.13$

TABLE I. Single electron energies, hopping parameters, $J(P)$ and δ for orthorhombic La214 (all values except the connecting vectors in eV). Here x^2 , z^2 , p_x , p_y , p_z denote Cu- $d_{x^2-y^2}$, Cu- $d_{3z^2-r^2}$, O- p_x , O- p_y , O- p_z orbitals respectively.

Parameters	Connecting vectors	3%-compr. along c axis	Undeformed material	3%-hydrostatic compr.
ϵ_{x^2}		-2.031	-1.849	-1.578
$\epsilon_{x^2} - \epsilon_{z^2}$		0.119	0.225	0.204
$\epsilon_{x^2} - \epsilon_{p_x}$		0.983	0.957	1.004
$\epsilon_{x^2} - \epsilon_{p_y}$		0.983	0.957	1.004
$\epsilon_{x^2} - \epsilon_{p_z}$		-0.503	-0.173	-0.311
$t(x^2, x^2)$	(-0.493,-0.5)	-0.173	-0.188	-0.215
$t(z^2, z^2)$	(-0.493,-0.5)	0.050	0.054	0.062
$t(x^2, p_x)$	(0.246,0.25,-0.02)	1.302	1.355	1.527
$t(z^2, p_x)$	(0.246,0.25,-0.02)	-0.547	-0.556	-0.618
$t(z^2, p_z)$	(0,0.04,0.445)	0.851	0.773	0.875
$t(p_x, p_y)$	(0.493, 0.0)	-0.854	-0.858	-0.935
$t'(p_x, p_y)$	(0,0.5,0.041)	0.757	0.793	0.862
$t(p_x, p_z)$	(-0.246,-0.21,0.465)	-0.447	-0.391	-0.423
$t'(p_x, p_z)$	(0.246,0.29,-0.425)	-0.424	-0.377	-0.408
$J(\Delta J\%)$		0.14(-5.7%)	0.15	0.18(19.9%)
δ_s		0.82	1.33	1.45

^{16,17} obtained in experiments on the two-magnon Raman scattering, but the one agrees well with the $J = 0.146$ eV from the neutron experiments.⁴⁵ In contrast under the uniaxial 3% compression along the c-axis $J(P_c)$ decreases by -5.7%, i.e. the superexchange constant changes much weaker. In both cases, the hydrostatic and anisotropic compression the superexchange constant $J(P)$ correlates with the in-plane hopping parameters and dd -excitation energy $\delta_s = \epsilon(^3B_1) - \epsilon(A_1)$ involving the two-hole states: Zhang-Rice state A_1 and triplet state 3B_1 (see Tab.I).

As shown on Fig.6 the antiferromagnetic character of superexchange is maintained even at a hypothetical set of Hamiltonian parameters corresponding the $A_1 \leftrightarrow ^3B_1$ - singlet-triplet crossover.

V. CONCLUSIONS

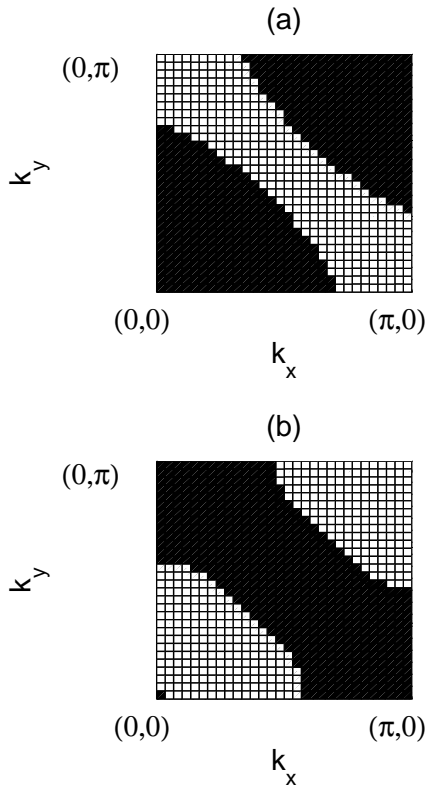


FIG. 5. (a) and (b): \vec{k} -dependence of the $\text{sign}(\delta A_{tot}(P))$ at the 3% - hydrostatic and uniaxial compressions respectively. Black area: (+), white: (-).

To sum up, using LDA+GTB approach we can describe the different pressure dependences $J(P)$ in the undoped La214 and qp -spectra on the same footing.

It is to be stressed that a pressure dynamics of the electron structure and superexchange interaction for the La214 is quite different under the hydrostatic and uniaxial (along c -axis) compressures. As shown on Fig.5 the \vec{k} -dependence of the $\text{sign}(\delta A_{tot})$ -function qualitatively reproduces the distribution of a_1 - and b_1 -orbital groups over the Brillouin zone. Thus the signs in the photocurrent changes are reversed at the different compressures. Nonetheless the total photoemission from the frs -state:

$\int \int A_{tot}(\vec{k}, E, P) \partial E \partial \vec{k}$ integrated over the energy window $\Delta E_{frs} \sim 1\text{eV}$ slightly decreases by -1.7% and -2.4% under the hydrostatic and uniaxial compressures respectively. Eventually the total photoemission depends on a width of energy window.

Thus even a simple hydrostatic effect on the electronic structure of the anisotropic antiferromagnetic La214 can provide us with useful information about a symmetry of the electronic states. However, currently we do not know anything about the possibilities of a photoemission spectroscopy under a pressure.

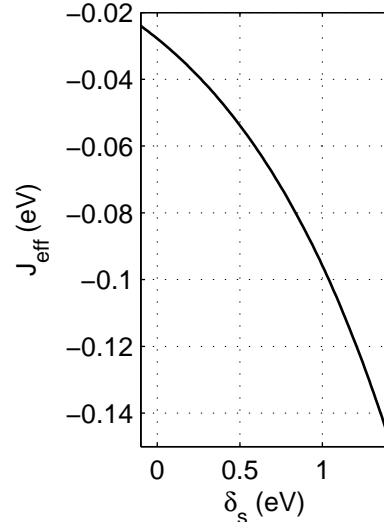


FIG. 6. A dependence of the superexchange interaction J_{eff} on the energy of dd -excitation δ_s at the Hamiltonian parameters corresponding to a crossover between the two-hole A_1 singlet and 3B_1 triplet states.

A comparison with results for the pressure dynamics of T_c near optimal hole doping reveals the universal trend of superexchange $J(P)$ together with the $T_c(P)$: $\partial J/\partial P > 0$ for isotropic pressure and $\partial J/\partial P_c < 0$ for anisotropic one. The last point is one more argument to the discussion on a nature of the pairing mechanism. At least at the optimal doping, we conclude that the behavior $J(P)$ is representative of the magnetic pairing interaction in the single CuO_2 layer cuprates.

Calculated by the LDA+GTB method the superexchange interaction $J \approx 0.15\text{eV}$ in the undeformed La214 agrees well with the $J = 0.146\text{eV}$ from neutron experiments.⁴⁵ The $J(P)$ increases by $\sim 20\%$ under hydrostatic 3%-compression. In contrast decreasing by $\sim -5.7\%$ the J changes much weaker under uniaxial 3% compression along the c -axis. In both cases, the hydrostatic and anisotropic compression the superexchange constant J correlates with the in-plane hopping parameters and the dd -excitation energy δ_s . In fact, at the $\sim 205\text{Kbar}$ hydrostatic pressure, the r_{Cu-O} reduces by the -3%,⁵¹ while the J increases by $\sim 18\%$.¹⁷

Due to the orbital features of the Zhang-Rice state (the same orbitals give the largest contribution to this state and pd -hopping) the superexchange J keeps the antiferromagnetic character even at a hypothetical set of Hamiltonian parameters corresponding a crossover of the Zhang-Rice singlet and first excited triplet states (Fig. 6).

ACKNOWLEDGMENTS

This work was supported by: program of fundamental research of the Russian Academy of Sciences "Quantum mesoscopic and disordered structures" 12-II -2-1002, President of Russia grant Sh-1044.2012.2 and GK

16.740.12.0731, Presidium of Russian Academy of Science Program 2.16, Siberian and Ural Branch of Russian Academy of Science Projects 44 and 97, RFFI grants: 11-02-00147, RFFI 12-02-31331, 13-02-01395, 13-02-00358 and Siberian Federal University grant F11.

-
- ¹ A. Lanzara, P. V. Bogdanov, X. J. Zhou, S. A. Kellar, D. L. Feng, E. D. Lu, T. Yoshida, H. Eisaki, A. Fujimori, K. Kishio, J.-I. Shimoyama, S. U. T. Noda, Z. Hussain, and Z.-X. Shen, *Nature* **412**, 510 (2001).
- ² J. Hwang, T. Timusk, and G. D. Gu, *Nature* **427**, 714 (2004).
- ³ J. Lee, K. Fujita, K. McElroy, J. A. Slezak, M. Wang, Y. Aiura, H. Bando, M. Ishicado, T. Masui, J.-X. Zhu, A. V. Balatsky, H. Eisaki, S. Ushida, and J. C. Davis, *Nature* **442**, 546 (2006).
- ⁴ J. P. Carbotte, E. Schachinger, and D. N. Basov, *Nature* **401**, 354 (1999).
- ⁵ E. Demler and S.-C. Zhang, *Nature* **396**, 733 (1998).
- ⁶ A. Abanov, A. V. Chubukov, M. Eschrig, M. R. Norman, and J. Schmalian, *Phys. Rev. Lett.* **89**, 177002 (2002).
- ⁷ D. J. Scalapino, *Rev. Mod. Phys.* **84**, 1383 (2012).
- ⁸ T. Cuk, F. Baumberger, D. H. Lu, N. Ingle, X. J. Zhou, H. Eisaki, N. Kaneko, Z. Hussain, T. P. Devereaux, N. Nagaosa, and Z.-X. Shen, *Phys. Rev. Lett.* **93**, 117003 (2004).
- ⁹ F. Hardy, N. J. Hillier, C. Meingast, D. Colson, Y. Li, N. Barisic, G. Yu, X. Zhao, M. Greven, and J. S. Schilling, *Phys. Rev. Lett.* **105**, 167002 (2010).
- ¹⁰ J. D. Jorgensen, D. G. Hinks, O. Chmaissem, D. N. Argyriou, J. F. Mitchell, and B. Dabrowski, "Recent developments in high temperature superconductivity," (Springer Berlin Heidelberg, 1996) pp. 1–15.
- ¹¹ H. Sakakibara, H. Usui, K. Kuroki, R. Arita, and H. Aoki, *Phys. Rev. Lett.* **105**, 057003 (2010).
- ¹² Y. Ohta, T. Tohyama, and S. Maekawa, *Phys. Rev. Lett.* **66**, 1228 (1991).
- ¹³ L. F. Feiner, J. H. Jefferson, and R. Raimondi, *Phys. Rev. Lett.* **76**, 4939 (1996).
- ¹⁴ E. Pavarini, I. Dasgupta, T. Saha-Dasgupta, O. Jepsen, and O. K. Andersen, *Phys. Rev. Lett.* **87**, 047003 (2001).
- ¹⁵ S. D. Conte, C. Giannetti, G. Coslovich, F. Cilento, D. Bossini, T. Abebaw, F. Banfi, G. Ferrini, H. Eisaki, M. Greven, A. Damascelli, D. van der Marel, and F. Parmigiani, *Science* **335**, 1600 (2012).
- ¹⁶ M. C. Aronson, S. B. Dierker, B. S. Dennis, S.-W. Cheong, and Z. Fisk, *Phys. Rev. B* **44**, 4657 (1991).
- ¹⁷ M. I. Eremets, A. V. Lomsadze, V. V. Struzhkin, A. A. Maksimov, A. V. Puchkoov, and I. I. Tartakovskii, *JETP Lett.* **54**, 372 (1991).
- ¹⁸ J. S. Schilling, "Handbook of high temperature superconductivity: Theory and experiment," (Springer Verlag, Hamburg, 2007) Chap. High Pressure Effects, Chapter 11, cond-mat/0008070.
- ¹⁹ V. Varma, S. Schmitt-Rink, and E. Abrahams, *Solid State Communications* **62**, 681 (1987).
- ²⁰ V. J. Emery, *Phys. Rev. Lett.* **58**, 2794 (1987).
- ²¹ H. Eskes and J. H. Jefferson, *Phys. Rev. B* **48**, 9788 (1993).
- ²² J. H. Jefferson, H. Eskes, and L. F. Feiner, *Phys. Rev. B* **45**, 7959 (1992).
- ²³ L. F. Feiner, J. H. Jefferson, and R. Raimondi, *Phys. Rev. B* **53**, 8751 (1996).
- ²⁴ V. A. Gavrichkov and S. G. Ovchinnikov, *Physics of the Solid State* **50**, 10811086 (2008).
- ²⁵ H. Kamimura, *Jpn. J. Appl. Phys.* **26**, L627 (1987).
- ²⁶ H. Kamimura and M. Eto, *J. Phys. Soc. Jpn* **59**, 3053 (1990).
- ²⁷ H. Eskes and G. A. Sawatzky, *Phys. Rev. B* **44**, 9656 (1991).
- ²⁸ J. B. Grant and A. K. McMahan, *Phys. Rev. Lett* **66**, 488 (1991).
- ²⁹ Y. Ohta, T. Tohyama, and S. Maekawa, *Phys. Rev. B* **43**, 2968 (1991).
- ³⁰ S. G. Ovchinnikov, V. A. Gavrichkov, M. M. Korshunov, and E. I. Shneyder, "Springer series in solid-state sciences," (Springer Berlin Heidelberg, Hamburg, Volume 171, 2012) Chap. LDA+GTB method for band structure calculations in the strongly correlated materials. In the Theoretical Methods for strongly Correlated systems, pp. 143–171, cond-mat/0008070.
- ³¹ K. C. Johnson and A. J. Sievers, *Phys. Rev. B* **10**, 1027 (1974).
- ³² T. Kaneko, H. Yoshida, S. Abe, H. Morita, K. Noto, and H. Fujimori, *Jpn. J. Appl. Phys.* **26**, L1374 (1987), and references therein.
- ³³ H. J. Kim and R. Moret, *Physica C: Superconductivity and Its Applications (Amsterdam, Netherlands)* **156**, 363 (1988).
- ³⁴ M. J. Massey, N. H. Chen, J. W. Allen, and R. Merlin, *Phys. Rev. B* **42**, 8776 (1990).
- ³⁵ F. C. Zhang and T. M. Rice, *Phys. Rev. B* **37**, 3759 (1988).
- ³⁶ S. Maekawa, T. Tohyama, S. E. Barnes, S. Ishibara, W. Koshibae, and G. Khaliullin, "Springer series in solid-state sciences," (Springer Verlag, Hamburg, 2004) Chap. Physics of Transition Metal Oxides.
- ³⁷ D. W. Smith, *J. Chem. Phys.* **50**, 2784 (1969).
- ³⁸ N. Fuchikami, *J. Phys. Soc. Jpn.* **28**, 871 (1970).
- ³⁹ L. J. de Jough and R. Block, *Physica B* **79**, 568 (1975).
- ⁴⁰ K. N. Shrivastava and V. Jaccarino, *Phys. Rev. B* **13**, 299 (1976).
- ⁴¹ U. Venkateswaran, K. Syassen, H. Mattausch, and E. Schonherr, *Phys. Rev* **38**, 7105 (1989).
- ⁴² H. Eskes, G. A. Sawatzky, and L. F. Feiner, *Physica C* **160**, 424 (1989).
- ⁴³ E. B. Stechel and D. R. Jennison, *Phys. Rev. B* **38**, 4632 (1988).
- ⁴⁴ J. F. Annett, R. M. Martin, A. K. McMahan, and S. Satpathy, *Phys. Rev. B* **40**, 2620 (1989).
- ⁴⁵ R. Coldea, S. M. Hayden, G. Aeppli, T. G. Perring, C. D. Frost, T. E. Mason, S. W. Cheong, and Z. Fisk, *Phys. Rev. Lett.* **86**, 5377 (2001).
- ⁴⁶ Y. B. Gaididei and V. M. Loktev, *Phys. Status Solidi B* **147**, 307 (1988).

- ⁴⁷ M. M. Korshunov, V. A. Gavrichkov, S. G. Ovchinnikov, I. A. Nekrasov, Z. V. Pchelkina, and V. I. Anisimov, Phys. Rev. B. **72**, 165104 (2005).
- ⁴⁸ V. A. Gavrichkov and S. G. Ovchinnikov, Phys. Solid State **40**, 163 (1998).
- ⁴⁹ S. G. Ovchinnikov and V. V. Val'kov, *Hubbard operators in the theory strongly correlated electrons* (Imperial College Press, London, 2004) p. 241.
- ⁵⁰ K. A. Chao, J. Spalek, and A. M. Oles, Journal of Physics C: Solid State Physics **10**, L271 (1977).
- ⁵¹ M. J. Akhar, C. R. A. Catlow, S. M. Clark, and W. M. Temmerman, J. Phys. C:Solid State Phys. **21**, L917 (1988).